The Astrophysical Journal, 623:362–371, 2005 April 10

DOWNSCATTERING DUE TO WIND OUTFLOWS IN COMPACT X-RAY SOURCES: THEORY AND INTERPRETATION

Lev Titarchuk[1,2] and Chris Shrader[2,3]
Received 2004 May 10; accepted 2004 August 4

ABSTRACT

A number of recent lines of evidence point toward the presence of hot, outflowing plasma from the central regions of compact Galactic and extragalactic X-ray sources. In addition, it has long been noted that many of these sources exhibit an "excess" continuum component above ~10 keV, usually attributed to Compton reflection from a static medium. Motivated by these facts, as well as by recent observational constraints on the Compton reflection models, specifically apparently discrepant variability timescales for line and continuum components in some cases, we consider possible effects of outflowing plasma on the high-energy continuum spectra of accretion-powered compact objects. We present a general formulation for photon downscattering diffusion that includes recoil and Comptonization effects due to divergence of the flow. We then develop an analytical theory for the spectral formation in such systems that allows us to derive formulae for the emergent spectrum. Finally, we perform the analytical model fitting on several Galactic X-ray binaries. Objects that have been modeled with high–covering-fraction Compton reflectors, such as GS 1353−64, are included in our analysis. In addition, Cyg X-3, which is widely believed to be characterized by dense circumstellar winds with temperature of the order of 10^6 K, provides an interesting test case. Data from *INTEGRAL* and *RXTE* covering the ~3–300 keV range are used in our analysis. We further consider the possibility that the widely noted distortion of the power-law continuum above 10 keV may in some cases be explained by these spectral softening effects.

Subject headings: accretion, accretion disks — black hole physics — radiation mechanisms: nonthermal — stars: individual (Cygnus X-1, Cygnus X-3, GS 1353−64, GX 339−4)

1. INTRODUCTION

Recent observational and theoretical evidence suggests that accretion-powered X-ray sources, of both the Galactic and extragalactic variety, may exhibit outflowing plasma, i.e., winds, emanating from a compact region near the central source (e.g., Elvis 2004; Arav 2004; Brandt & Schulz 2000; Proga & Kallman 2002). Comptonization effects in those putative outflows are likely to alter the intrinsic continuum spectra of accretion-powered compact objects. The basic idea is that electron scattering of photons from a central source entering the expanding outflow causes a decrease in energy (downscattering). The magnitude of this decrease is of first order in v/c and in $E/m_e c^2$, where v is the outflow speed, c is the speed of light, E is the initial photon energy, and m_e is the electron rest mass.

The basic idea is depicted in Figure 1. There we present a simple explanation of the diverging flow effect on the photon propagation through the medium. A photon emitted outward near the inner boundary and then scattered at a certain point by an electron moving with velocity $\boldsymbol{v}_1$ is received by an electron moving with velocity $\boldsymbol{v}_2$, as shown, with frequency $\nu_2 = \nu_1[1 + (\boldsymbol{v}_1 - \boldsymbol{v}_2)\cdot\boldsymbol{n}/c]$, where $\boldsymbol{n}$ is a unit vector along the path of the photon at the scattering point. In a diverging flow $(\boldsymbol{v}_1 - \boldsymbol{v}_2)\cdot\boldsymbol{n}/c < 0$, and photons are successively redshifted until scattered to an observer at infinity. The color of the photon path (in Fig. 1) indicates the frequency shift in the rest frame of the receiver (electron or the Earth observer). On the other hand, referring to the right-hand side of Figure 1, in a converging flow $(\boldsymbol{v}_1 - \boldsymbol{v}_2)\cdot\boldsymbol{n}/c > 0$, and photons are blueshifted.

The classical Compton (recoil) effect $\langle \Delta E \rangle / E \sim -E/m_e c^2$ has been well understood for a long time. Basko et al. (1974) first studied the downscattering effects in the interaction of X-ray radiation of the central source with the relatively cold atmosphere of the optical companion in a binary system. They predicted the shape of the X-ray reflection spectrum of the companion and applied these results to the Her X-1 system. X-ray observations of Her X-1 by a number of groups (e.g., Sheffer et al. 1992; Still et al. 2001) confirmed this prediction. In particular, the numerical calculations by Basko et al. (1974) demonstrated that the reflection of the bremsstrahlung spectrum distorted the high-energy continuum above 10 keV, producing the characteristic continuum excess feature, or "bump," in the >10 keV spectrum. This feature was also identified by Sunyaev & Titarchuk (1980, hereafter ST80), who found that the transmitted, downscattered spectrum is formed as a result of the reprocessing of X-ray radiation from the central source in an ambient spherical cloud. From these facts one can conclude that this distortion of the continuum is not an intrinsic property of the particular incident photon distribution, but it is rather a result of downscattering effects from X-ray photons diffusing through the intervening medium.

In this paper we show that this is precisely the case. We formulate the problem of the photon diffusion in generic terms and demonstrate a specific solution for bulk motion in which effects of a recoil and divergence of the flow are taken into account. The emergent spectrum as an outcome of this solution has all these aforementioned features of the downscattering.

The details of the radiative transfer problem taking into account downscattering effects (recoil and Doppler effect in the

[1] Center for Earth Observing and Space Research, George Mason University, Fairfax, VA 22030; and US Naval Research Laboratory, Code 7655, Washington, DC 20375-5352; ltitarchuk@ssd5.nrl.navy.mil.
[2] NASA Goddard Space Flight Center, Code 660, Greenbelt, MD 20771; lev@lheapop.gsfc.nasa.gov, Chris.R.Shrader@gsfc.nasa.gov.
[3] Universities Space Research Association, 7501 Forbes Boulevard, Seabrook, MD 20706.

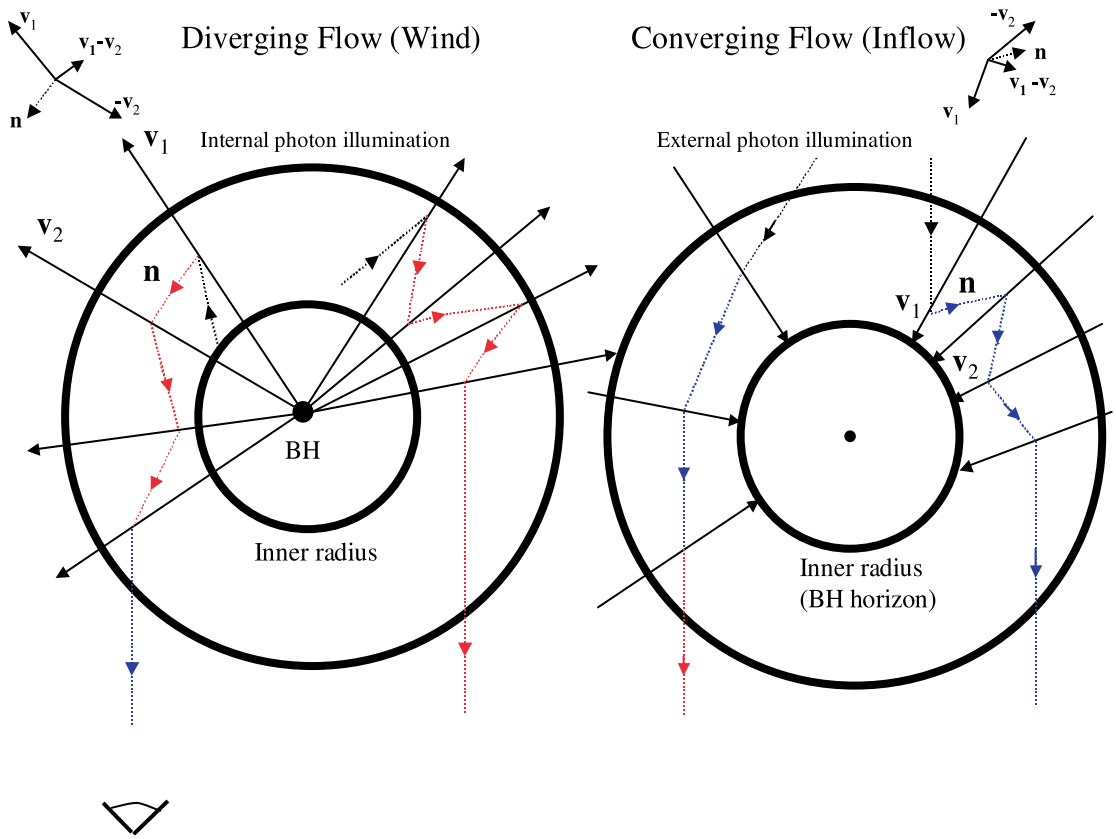

FIG. 1.—*Left*: Schematic diagram depicting the wind geometry. The outflow (wind) originates at the inner radius. The electron optical depth of the wind is of order unity. A photon emitted near the inner boundary and subsequently scattered by an electron moving with velocity $\boldsymbol{v}_1$ impinges on an electron moving with velocity $\boldsymbol{v}_2$ as shown. The change in frequency is $\nu_2 = \nu_1[1 + (\boldsymbol{v}_1 - \boldsymbol{v}_2)\cdot\boldsymbol{n}/c]$, where $\boldsymbol{n}$ is a unit vector along the path of the photon at the scattering point. In a diverging flow $(\boldsymbol{v}_1 - \boldsymbol{v}_2)\cdot\boldsymbol{n}/c < 0$, and photons are successively redshifted until scattered to an observer at infinity. The color of the photon path indicates the frequency shift in the rest frame of the receiver (electron or the Earth observer). *Right*: In a converging flow $(\boldsymbol{v}_1 - \boldsymbol{v}_2)\cdot\boldsymbol{n}/c > 0$, and photons are blueshifted.

divergent flow) and its solution are given in § 2. In § 3, we apply our model to observational data for several Galactic X-ray binaries. We attempt to demonstrate the Compton downscattering effects in relatively cold outflows, for which temperature is of the order of 10^6 K, and disk atmospheres, which are necessary constituents of X-ray sources. For example, Cygnus X-3, which is believed to be characterized by dense circumstellar (or circumdisk) winds, provides an interesting test case. A number of additional sources that have been noted in the literature to exhibit evidence for strong "Compton reflection," e.g., GS 1353−64 and GX 339−4, have also been included in our analysis. We consider the possibility that this well-documented distortion of the power-law continuum above 10 keV may in some cases be due to downscattering from outflowing plasma rather than from a static reflecting media. We further speculate that this could possibly apply to extragalactic (i.e., active galactic nuclei [AGNs]) as well as Galactic accretion objects (§ 4), although we do not present any analysis of AGNs here. A summary and conclusions follow in § 5.

2. RADIATIVE TRANSFER IN A BULK OUTFLOW

2.1. *The Basic Downscattering Problem*

The problem of photon propagation in a fluid in bulk motion has been studied in detail in a number of papers (see, e.g., Blandford & Payne 1981; Payne & Blandford 1981; Nobili et al. 1993; Titarchuk et al. 1997; Titarchuk et al. 2003, hereafter TKB03; Laurent & Titarchuk 1999, 2001; Laurent & Titarchuk 2004, hereafter LT04). In particular, TKB03 present a general formulation and a solution of the spectral formation in the diverging outflow. They demonstrated that the resulting spectrum can be formed as a convolution of energy and space diffusion solutions. The spread function, given by a Green's function formulation, applied to a monochromatic injection yields a redshift-skewed line that is a power law at low energies. Furthermore, Monte Carlo simulations show that the line width has a strong dependence on v/c, optical depth τ, and the energy of the monochromatic line E_0 only when the flow temperature $kT_e < 1$ keV (LT04). TKB03 and LT04 also establish that the shape of the spectral line should be closely related to the photon source distribution in the flow. Comparison of the theoretical spectra with data shows that observed red-skewed lines are formed as a result of transmission of the X-ray radiation through outflows of moderate Thomson optical depth ($\tau_0 \gtrsim 1$).

To apply these radiative transfer results to observational data, we have developed a generic analytical formulation that leads to a simple analytic expression for modification of the emergent spectrum due to recoil and velocity divergence effects in the flow. For the recoil effect, we extend the results of ST80, who show that the downscattering feature, or "bump," can appear superposed on power-law spectra with indices $\alpha < 1$ as a result of photon diffusion through a static cloud. From ST80 and calculations presented here, one might conclude such bumps are not a necessarily a feature of disk reflection, but could instead be a generic feature of the photon

reprocessing in a relatively cool, ambient plasma characterized by temperatures of the order of 10^6 K.

2.2. *Main Equations and Solution of Downscattering Problem*

Let $N(r) = N_0(r_0/r)^b$ be the radial number density profile of an outflow, and let its radial outward speed be

$$v_b/c = (\dot{M}_{\rm out}/4\pi c m_p N_0 r_0^2)(r_0/r)^{2-b} = v_0(r_0/r)^{2-b}, \quad (1)$$

obtained from mass conservation in a spherical geometry (here $\dot{M}_{\rm out} = 4\pi r^2 v_b m_p N$, and m_p is the proton mass). The Thomson optical depth of the flow from some radius r to infinity is given by

$$\tau = \int_r^\infty N_e(r)\sigma_{\rm T}\, dr = \sigma_{\rm T} N_0 r_0 (r_0/r)^{b-1}/(b-1), \quad (2)$$

where $N_e(r) = N(r)$ is the electron density, $\sigma_{\rm T}$ is the Thomson cross section, and r_0 is a radius at the base of the outflow. Because our final results are independent of the velocity and density profiles, we use $b = 2$ (a constant-velocity outflow) below for simplicity of presentation. In this case $\tau_0 = \tau(r_0) = \sigma_{\rm T} N_0 r_0$.

The transfer of radiation within the flow in space and energy is governed by the photon kinetic equation (Blandford & Payne 1981, eq. [18]) for the photon occupation number $n(r, \nu)$, which in steady state reads

$$-\frac{\boldsymbol{v}_b/c}{\kappa}\cdot\nabla n + \frac{1}{3\kappa}\nabla\cdot\left(\frac{1}{\kappa}\nabla n\right) + \frac{1}{3}\frac{\nabla\cdot(\boldsymbol{v}_b/c)}{\kappa}\, z\frac{\partial n}{\partial z} + \frac{1}{z^2}\frac{\partial(z^4 n)}{\partial z} = -j(r,\nu), \quad (3)$$

where $z = h\nu/m_e c^2$ is the dimensionless photon energy, $\kappa = N_e(r)\sigma_{\rm T}$ is the inverse of the scattering mean free path, $\boldsymbol{v}_b = v_b \boldsymbol{e}_r$ is the flow velocity, $\boldsymbol{e}_r$ is the radial unit vector, and $j(r, \nu)$ is the photon source term.

The spectral flux $F(r, \nu)$ (Payne & Blandford 1981) is given in terms of $n(r, \nu)$ by

$$F(r,\nu) = -\frac{1}{3\kappa(r)}\nabla n - \frac{1}{3} v_b\, \nu\frac{\partial n}{\partial \nu}, \quad (4)$$

and must satisfy the following boundary conditions: (1) conservation of the frequency-integrated flux over the outer boundary,

$$L_r^{(1)} n = \int F(r,\nu)\, d\nu \propto r^{-2} \text{ as } r \to \infty; \quad (5)$$

and (2) in terms of the specific intensity of the radiation, the escaping radiation from the inner boundary be equal to the radiation entering the wind shell through the inner boundary (see Fig. 1 for the wind geometry). We neglect here the possible absorption of the radiation at the central source (black hole). Thus the occupation number should satisfy some kind of reflection condition at the inner boundary $r = r_0$, namely, the photon flux at the inner boundary should be zero (all photons scattered in the outflow shell and escaped through the inner boundary subsequently return), i.e.,

$$L_r^{(2)} n(r_0) = 0. \quad (6)$$

In this formulation of the problem the number of photons emitted in the wind shell is equal to that escaped to the Earth observer (i.e., the photon number is conserved). This can be proven using equations (3)–(5).

Consequently, if the escaping high-energy photons lose their energy but the number of photons is conserved, *there must be accumulation of the photons at a particular lower energy band.* This accumulation effect was previously noted by ST80 for the case in which the photon energy loss (downscattering) was determined by the recoil effect only (see Fig. 10 in ST80). In § 2.3 we demonstrate this accumulation effect when the recoil and flow divergence dowscattering effects are taken into account.

It is worth noting that in TKB03 the goal was to demonstrate the pure effect of the flow divergence on a spectral line as a result of multiple scatterings with the plasma free electrons. They thus omitted the recoil term in the left-hand side of equation (3). They were also interested in applying their solution to the spectral formation of iron lines, for which photon energies are about 6.4 keV and lower. For such energies the recoil effect can be safely neglected (see ST80). On the other hand, if one is interested in the modification of the continuum spectrum at energies higher than 10 keV by multiple downscattering events in the "cold" medium, this effect must be taken into account. Below, we show how one can generalize the TKB03 solution including the recoil term in the radiative transfer equation. We apply a particular method for the separation of variables suggested in Titarchuk (1994, hereafter T94) and successfully used in TKB03 to obtain our solution.

In order to further proceed with the solution derivation we should note that Laurent & Titarchuk (2004) find that the coefficient in the diverging term of equation (3), $\tilde{\varepsilon} = \nabla\cdot(\boldsymbol{v}_b/c)/\kappa$, can be replaced by a constant $\tilde{\varepsilon}$. Strictly speaking, $\tilde{\varepsilon}$ is a function of r and consequently of τ; $\tilde{\varepsilon} = 2(v_b/c)/\tau$.

Using the Fokker-Planck equation (see eq. [3] in TKB03) and a method developed by Titarchuk et al. (1997; see their Appendix D), one can relate the mean energy change per scattering $\langle \Delta E\rangle$ for photons undergoing numerous scatterings in the flow to $\beta = v/c$:

$$\langle \Delta E\rangle \approx -[f\nabla\boldsymbol{v}/(c\kappa)]E \approx -(2f\beta/\tau_0)E, \quad (7)$$

where $\boldsymbol{v} = v\boldsymbol{e}_r$ is the flow velocity, $\boldsymbol{e}_r$ is the radial unit vector, and $\kappa = N_e\sigma_{\rm T}$ is the inverse of scattering mean free path l. The numerical factor f in formula (7) is of order unity, and LT04 obtain its precise value using their Monte Carlo simulations.

In LT04 (specifically, Fig. 2 of that paper) the escape photon distribution $\varphi(t)$ for five energy bands is presented. In the plot the time is given in light crossing time units $t_{\rm cross} = \Delta r/c$, where Δr is the outflow cloud thickness. Photons that escape without any scattering are at 6.6 keV. The model parameters are $kT_e = 0.1$ keV, $\tau_0 = 4$, and $\beta = v/c = 0.1$.

The simulated time distribution is fitted by an exponential $\varphi(t) = C_N \exp(-at/t_{\rm cross})$, where a is equal to 0.67, identical to that predicted by diffusion theory (see Sunyaev & Titarchuk 1985, hereafter ST85). ST85 show that the average number of scatterings $N_{\rm av}$ in the shell of optical depth τ_0 is $3\tau_0^2/8$, so the average photon-scattering time is $t_{\rm av} = N_{\rm av} l/c = 3\tau_0 t_{\rm cross}/8$, where $l = 1/N_0\sigma_{\rm T} = \Delta r/\tau_0$. ST85 also show that the time distribution for scattered photons in any bounded medium is an exponential, $\varphi(t) = C_N \exp(-t/t_{\rm av})$, where $C_N = 1/t_{\rm av}$ $\left[\int_0^\infty f(t)dt = 1.\right]$

In this particular case

$$f(t) = C_N \exp\left(-\frac{t}{t_{\rm av}}\right) = C_N \exp\left[-\frac{2}{3}\frac{t}{(\tau_0/4)\, t_{\rm cross}}\right],$$

precisely what is obtained in the LT04 simulations. Thus, the average energy of photons escaping after $N_{\rm av}$ scatterings is $\langle E\rangle_{\rm sc} \approx (1 + \langle \Delta E\rangle)^{N_{\rm av}}$. Using formula (7) one can obtain

$$\langle E\rangle_{\rm sc} \approx (1 - 2f\beta/\tau_0)^{N_{\rm av}} E_0. \tag{8}$$

For the particular case of $\tau_0 = 4$ and $\beta = 0.1$, LT04 find that the original photon energy $E_0 = 6.6$ keV is reduced to $E_0 = 5.4$ keV after $N_{\rm av}$ scatterings in the outflow (the emergent spectrum is shown in Fig. 1 of LT04, left panel). The analytical estimate obtained from formula (8) is close to this value of $\langle E\rangle_{\rm sc} = 5.4$ keV for $f \approx 2/3$. Thus one considers an approximation in which the diverging term in equation (3) is independent of the space variable.

2.3. *Downscattering Solution: Emergent Spectrum*

According to a theorem (T94, Appendix A), the solution of any equation whose left-hand side operator acting on the unknown function $n(r, \nu)$ is the sum of two operators L_r and L_ν, which depend correspondingly only on space and energy and the right-hand side $j(r, \nu)$, can be factorized, i.e.,

$$L_r n + L_\nu n = -j(r, \nu) = -f(r)\varphi(\nu). \tag{9}$$

The boundary conditions are independent of the energy ν, i.e.,

$$L_r^{(1)} n = 0 \text{ as } r \to \infty, \quad L_r^{(2)} n = 0 \text{ for } r = r_0, \tag{10}$$

and n is given by the convolution of the solutions of the time-dependent problem of each operator,

$$n(r, \nu) = \int_0^\infty P(r, u) X(\nu, u)\, du. \tag{11}$$

Above, u is the dimensionless time (which can be the Thomson dimesionless time $u_{\rm T} = N_0 \sigma_{\rm T} c t$ depending on the specific forms of operators L_r and L_ν); $P(r, u)$ is the solution of the initial value problem of the spatial operator L_r,

$$\frac{\partial P}{\partial u} = L_r P, \quad P(r, 0) = f(r), \tag{12}$$

with boundary conditions

$$L_r^{(1)} P = 0 \text{ as } r \to \infty, \quad L_r^{(2)} P = 0 \text{ at } r = r_0; \tag{13}$$

and $X(\nu, u)$ is the solution of the initial value problem of the energy operator L_ν,

$$\frac{\partial X}{\partial u} = L_\nu X, \quad X(z, 0) = \varphi(z), \tag{14}$$

with boundary conditions

$$z^3 X \to 0 \text{ when } z \to 0, \infty. \tag{15}$$

Thus, we have

$$L_r P = -\frac{\boldsymbol{v}_b/c}{\kappa} \cdot \nabla P + \frac{1}{3\kappa} \nabla \cdot \left(\frac{1}{\kappa} \nabla P\right). \tag{16}$$

Following the LT04 arguments, we replace the coefficient of the diverging term by a constant $\varepsilon = 2q(v_b/c)/\tau_{\rm T,0} \ll 1$, where a numerical factor q is of order unity (see details in the end of § 2.2).

In the case in which the photon energy is due to a recoil effect and Comptonization effects in the diverging flow, we have

$$\frac{\partial X}{\partial u} = L_\nu X = \frac{1}{3}\varepsilon z \frac{\partial X}{\partial z} + \frac{1}{z^2}\frac{\partial (z^4 X)}{\partial z}, \tag{17}$$

where

$$X(z, 0) = \varphi(z)/z^3, \tag{18}$$

with boundary conditions

$$z^3 X \to 0 \text{ when } z \to 0, \infty. \tag{19}$$

We transform equation (17) introducing a new unknown function $Y = e^{(4\varepsilon/3)u} z^4 X$ for which equation (17) has a form

$$\frac{\partial Y}{\partial u} = \left(\frac{\varepsilon}{3} z + z^2\right) \frac{\partial Y}{\partial z}. \tag{20}$$

The problem for equation (20) with appropriate initial condition $Y(z, 0) = z\varphi(z)$ and boundary conditions $Y \to 0$ when $z \to 0, \infty$ is an initial value problem for the first-order partial differential equation, and it can be found using the method of characteristics (see, e.g., TKB03). The differential equation for the characteristics is

$$du = -\frac{dz}{(\varepsilon/3) z + z^2}. \tag{21}$$

That solution is

$$u = \frac{3}{\varepsilon}\left[\ln (z + \varepsilon/3)/z - \ln (z_0 + \varepsilon/3)/z_0)\right], \tag{22}$$

where z_0 is the dimensionless energy at $u = 0$. Because $Y(z_0, 0) = z_0 \varphi(z_0)$ is conserved along the characteristics, the solution of the problem for equations. (17)–(19) is

$$J(z, u) = z^3 X(z, u) = e^{-4\varepsilon u/3} \varphi[\psi_\varepsilon(z, u)]/[z \psi_\varepsilon(z, u)], \tag{23}$$

where

$$z_0 = \psi_\varepsilon(z, u) = (\varepsilon/3)/[(1 + \varepsilon/3z) \exp(-\varepsilon u/3) - 1]$$

is found from equation (22). Substitution of $J(z, u)$ from equation (23) into equation (11) gives us the emergent spectral shape,

$$\mathcal{F}_E(z, \varepsilon) = \left[\tau^{-2} F(\tau, z)\right]\Big|_{\tau \to 0} \propto \frac{1}{z}\int_0^{u_{\max,\varepsilon}(z)} e^{-4\varepsilon u/3} [\psi_\varepsilon(z, u)]^{-1} \varphi[\psi_\varepsilon(z, u)] \mathcal{P}(u)\, du, \tag{24}$$

where $u_{\max,\varepsilon}(z) = (3/\varepsilon)\ln(1+\varepsilon/3z) \gg 1$, and $\mathcal{P}(u) \propto \{\tau^{-2}[\partial P(\tau,u)/\partial\tau]\}|_{\tau\to 0}$ using the expressions for $F(\tau,z)$ and $P(\tau,u)$ (see eq. [4] and eqs. [12]–[13] for the definition of $F(\tau,z)$ and $P(\tau,u)$, respectively).

This result is a generalization of the results of ST80 and TKB03. ST80 derived the spectra when the downscattering effects due to the recoil were taken into account. On the other hand, TKB03 considered the downscattered spectra as a result of the divergence of the flow. For example, one can obtain ST80's formula (36) for the recoil spectrum assuming $\varepsilon \to 0$ in equation (24). In fact,

$$\lim_{\varepsilon\to 0}\psi_\varepsilon(z,u) = (1/z-u)^{-1},$$

and $u_{\max,0}(z) = 1/z$.

That formula (eq. [24]) for $\varepsilon = 0$ (the recoil case) is generic, and it is valid for any geometric configuration of the plasma cloud, e.g., a disk or a spherical cloud, as well as for any photon source distribution within the cloud, e.g., uniform or central illumination distributions. In fact, what we use here to derive this formula are the particular properties of the diffusion operator of the left-hand side of the main equation (eq. [9]), the boundary conditions (eq. [10]), and the source term in right-hand side of equation (9). Namely, we use that (1) the diffusion operator should be a sum of two operators: the space diffusion operator and the energy operator; (2) the boundary conditions are independent of energy; and (3) the source function is factorized [or presented as a linear superposition of the products of $f(r)\varphi(\nu)$]. All these mathematical properties are generic for the diffusion problem and independent of any specific geometry and spectral and space source distribution (see ST80 and T94 for more details and particular examples).

Below, we demonstrate how formula (24) can be simplified by exploiting the fact that the downscattering energy change $\Delta E/E$ is proportional to ε and E/m_ec^2.

It should be noted that modification of the spectrum occurs when photons undergo at least a few scatterings, namely, when the photon Thomson dimensionless time (or a number of scattering) $u > 1$. It is always on the order of the average number of scatterings

$$\tilde{N}_{\rm av} = \int_0^\infty u\mathcal{P}(u)\,du \Big/ \int_0^\infty \mathcal{P}(u)\,du.$$

Thus we can expand the integrand function,

$$W_\varepsilon(z,u) = e^{-4\varepsilon u/3}[\psi_\varepsilon(z,u)]^{-1}\varphi[\psi_\varepsilon(z,u)],$$

over u in formula (24) as

$$W(z,u)_\varepsilon \approx W_\varepsilon(z,0) + W'_\varepsilon(z,0)u. \tag{25}$$

This expansion is valid because we consider the case in which $N_{\rm av} \ll 1/\varepsilon$. ($\tau_{\rm T,0} \gtrsim 1$, $\varepsilon \ll 1$.) Substitution of equation (25) into equation (24) gives us

$$\mathcal{F}(\nu) \propto z^{-1}\left[W_\varepsilon(z,0) + N_{\rm av}W'_\varepsilon(z,0)\right], \tag{26}$$

where $z^{-1}W_\varepsilon(z,0)$ is the incident spectrum $\varphi(z)$, and

$$\frac{W'_\varepsilon(z,0)}{z} = \varphi(z)\left(\{\ln[z_0\varphi(z_0)]\}'_{z_0}\Big|_{u=0}\frac{\partial z_0}{\partial u}\Big|_{u=0} - \frac{4\varepsilon}{3}\right), \tag{27}$$

where

$$z_0 = \psi_\varepsilon(z,u) = \left(\frac{\varepsilon}{3}\right)\Big/\left[\left(1+\frac{\varepsilon}{3z}\right)\exp\left(-\frac{\varepsilon u}{3}\right) - 1\right],$$

and

$$\frac{\partial z_0}{\partial u}\Big|_{u=0} = z^2\left(1+\frac{\varepsilon}{3z}\right). \tag{28}$$

Substitution of equations (27), (28), and $\varphi(z) = z^{-1}W_\varepsilon(z,0)$ into equation (26) leads us to the formula

$$\mathcal{F}_E(z,\varepsilon) \propto \varphi(z)\left[1 - \left(\frac{4\varepsilon}{3}\right)\tilde{N}_{\rm av} + \tilde{N}_{\rm av}z^2\left(1+\frac{\varepsilon}{3z}\right)\{\ln[z_0\varphi(z_0)]\}'_{z_0}|_{u=0}\right]. \tag{29}$$

The most interesting case is the downscattering modification of the Comptonization spectrum (see, e.g., ST80; T94) that can be well fitted by a power-law spectrum with an exponential cutoff,

$$\varphi_{\rm Comp}(z) \approx z^{-\alpha}\exp(-z/z_*). \tag{30}$$

The cutoff energy E_* is related to the Compton cloud electron temperature kT_e by $E_* \approx 2kT_e$. For $\varphi_{\rm Comp}(z)$, it is evident that

$$\{\ln[z_0\varphi(z_0)]\}'_{z_0}|_{u=0} = (1-\alpha)/z - 1/z_*. \tag{31}$$

Using equation (31), we transform formula (29) as

$$\mathcal{F}_E(z,\varepsilon) \propto \varphi_{\rm Comp}(z)\left\{1 - \left(\frac{4\varepsilon}{3}\right)\tilde{N}_{\rm av} + \tilde{N}_{\rm av}z\left(1+\frac{\varepsilon}{3z}\right)\left[(1-\alpha) - \frac{z}{z_*}\right]\right\}. \tag{32}$$

The modification of the absolute normalization of the spectrum due to the downscattering effects is quite obvious: the relative change of the normalization is $1-(1+\alpha)\varepsilon\tilde{N}_{\rm av}/3$. Thus, we can rewrite equation (32) as the final formula for the spectral shape as

$$\mathcal{F}_E(z,\varepsilon) \propto \varphi_{\rm Comp}(z)\left\{1 + N_{\rm av}z\left[(1-\alpha) - \frac{\varepsilon}{3z_*} - \frac{z}{z_*}\right]\right\}, \tag{33}$$

where $N_{\rm av} = \tilde{N}_{\rm av}/[1-(1+\alpha)\varepsilon\tilde{N}_{\rm av}/3]$. The second term in parentheses of formula (33) describes the pileup and softening of the Comptonization spectrum $\varphi_{\rm Comp}(z)$ due to the downscattering effect in the outflow. In Figure 2*a* we present an $E\mathcal{F}_E$ diagram for various $N_{\rm av}$ and ε. The downscattering bump and softening of the spectrum are clearly seen in this plot (see also Fig. 2*b*, where a ratio of the Comptonization models to the incident spectrum [eq. (30)] is plotted).

Below, we apply formula (33) to the X-ray spectral data for a number of sources. The self-consistency of application of this formula for data fitting can be checked by comparison of the best-fit parameter $N_{\rm av}$ and $u_{\max,\varepsilon}(z_{\max})$ [the formula for $u_{\max,\varepsilon}(z)$ is shown just after eq. (24)]. Our inferred best-fit parameter $N_{\rm av} \ll u_{\max,\varepsilon}(z_{\max})$ for all fits, and thus our formula (33) as the

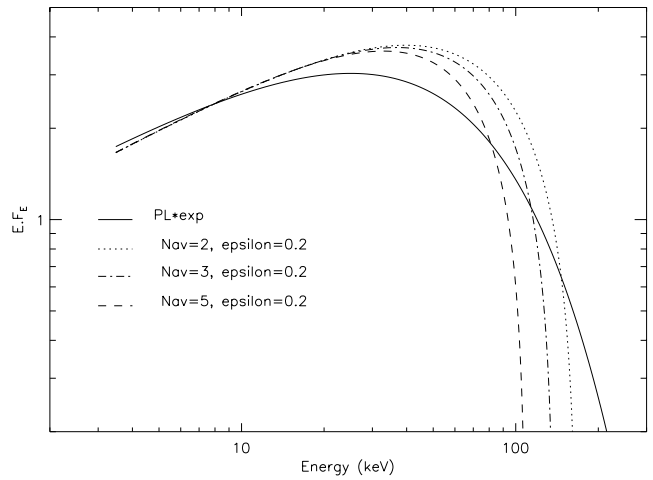

FIG. 2*a*

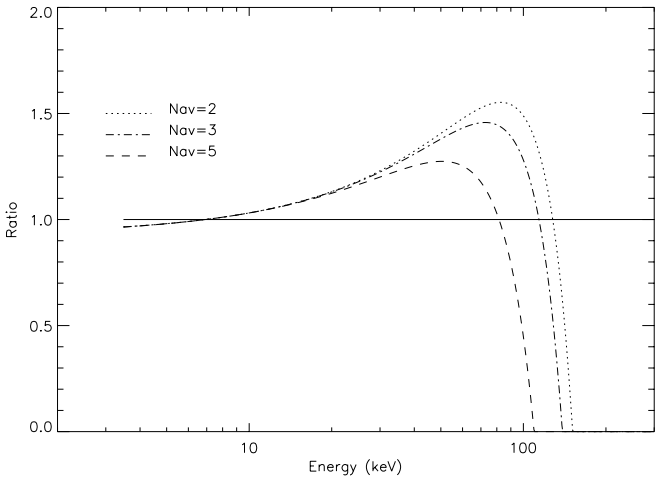

FIG. 2*b*

FIG. 2.—(*a*) $E\mathcal{F}_E$ diagram representing the thermal Comptonization spectra that result from photon propagation through a divergent outflow. The photon source is in the center of the outflow shell. *Solid line*: Emission of the central source for which a spectrum is $E^{-\alpha}\exp(-E/E_*)$, where $\alpha = 0.5$ and $E_* = 50$ keV. *Dashed, dot-dashed, and dotted lines*: Emission not escaping radiation from the outflow shell for average number of scattering $N_{\rm av} = 2$, 3, and 5, respectively. The effective coefficient of the outflow divergence $\varepsilon = 0.2$. (*b*) Similar to (*a*), except that a ratio of the Comptonization models to the exponentially cut off power-law spectrum is plotted.

analytical approximation of equation (24) is valid for all cases considered.

3. DATA ANALYSIS

To test these ideas we obtained public data from the *INTEGRAL* and HEASARC (*RXTE*) archives for a sample of Galactic X-ray binaries (Table 1). The Cygnus region was covered extensively by *INTEGRAL* in the early stages of that mission, the performance verification phase (2002 November–December), subsets of which are in the public domain at the time of this submission. Specifically, we selected coverage of Cyg X-3 and Cyg X-1 obtained during revolutions 22–25. Statistics are limited by the small amount of useful data, given the early problems with data gaps. We extracted spectra from JEM-X and SPI, using the OSA release version 3 software. Subsequent model fitting was done with the XSPEC spectral analysis package (ver. 12.10α) modified to include a local implementation of the model described in § 2. We also analyzed the JEM-X and SPI data for Cyg X-1, applying the same model. For comparison, we also obtained and analyzed contemporaneous *RXTE* data for both sources. In all cases, we used the *RXTE* calibration database and software release current as of 2004 April. We also used *RXTE* data for the additional sources GX 339−4 and GS 1354−63, each of which have been modeled by various other groups (e.g., Gilfanov et al. 1999; Nowak et al. 2002; Pottschmidt et al. 2003; Vilhu et al. 2003) as a power-law exponential plus a Compton "reflection" continuum (see, e.g., Magdziarz & Zdziarski 1995). For example, GS 1353−64 was found to require a large reflection continuum, $R \sim 0.3$–0.6 (Gilfanov et al. 2004). In addition to the Comptonized continuum, iron line structure—a Gaussian line component and absorption edge feature—was found to improve the quality of the fit at low energies. In addition, a systematic error component of 1% was added to the PCA data. We note that there is a significant cross-calibration discrepancy between the *INTEGRAL* SPI and JEM-X instruments (e.g., Paizis et al. 2003). We have assumed that the absolute flux calibration of SPI is reliable (Attié et al. 2003; Sturner et al. 2003) and renormalized the JEM-X model fits accordingly.

In Table 1 we list our source sample and the inferred parameters of the outflow Comptonization from our analysis. Here $\Gamma = \alpha + 1$ is the (photon) spectral index, and $N_{\rm av}$ is the average number of scatterings experienced by a typical photon in the outflow (§ 2). The origin of the data, *RXTE* (PCA plus HEXTE) or *INTEGRAL* (JEM-X plus SPI), is also indicated. We note that two Cyg X-3 observations represent very different intensity states for that source. For that matter, the GX 339−4 and GS 1353−64 observations used correspond to high-intensity states for each of those sources (but in this case, the spectral energy distributions represent the low-hard state).

In Figure 3, we present an E^2F_E versus E diagram (where F_E is a photon number in this case) to further illustrate the downscattering effect. Plotted there is our best-fit model curve, using GX 339−4 as a test case, compared to a simple exponentially folded power law fitted to the same data, with an accompanying

TABLE 1
SOURCE SAMPLE AND COMPTONIZATION MODEL PARAMETERS

Source ID	Observatory	Γ	$N_{\rm av}$	E_*	ϵ	Flux	χ^2_ν	Degrees of Freedom
Cyg X-1	*INTEGRAL*	1.74	0.8	175	0.12	10.01	1.544	1359
Cyg X-1	*RXTE*	1.51	1.7	219	0.12	17.1	1.651	80
GX 339−4	*RXTE*	1.63	3.2	299	0.10	4.27	0.988	123
GS 1353−64	*RXTE*	1.35	1.9	103	0.10	5.2	1.015	122
Cyg X-3	*INTEGRAL*	2.61	1.6	160	0.10	5.57	1.218	1550
Cyg X-3	*RXTE*	2.03	1.01	270	0.10	13.1	1.068	68

NOTE.—Flux is for 3–100 keV in units of 10^{-9} ergs cm^{-2} s^{-1}.

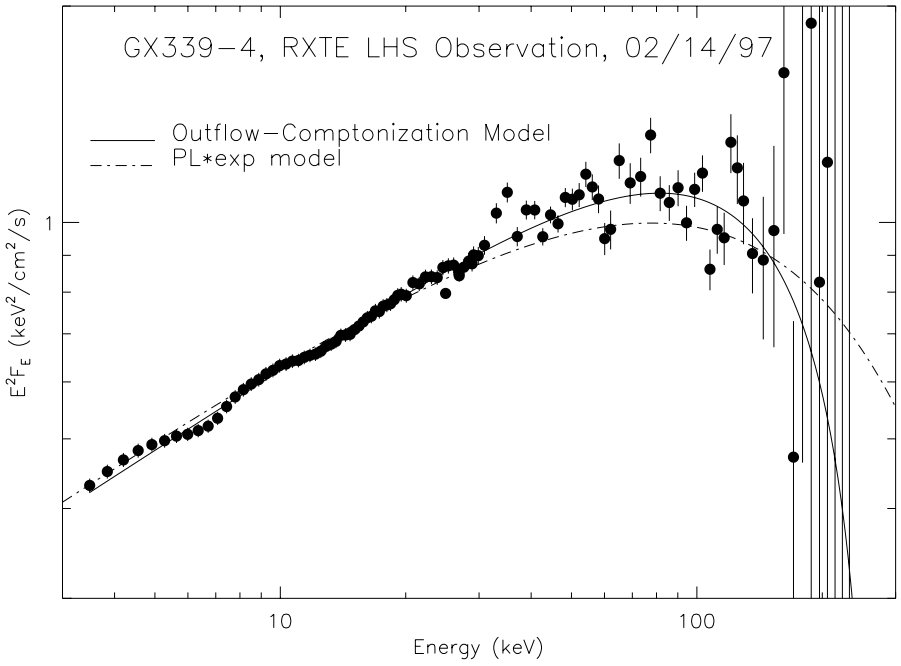

FIG. 3*a*

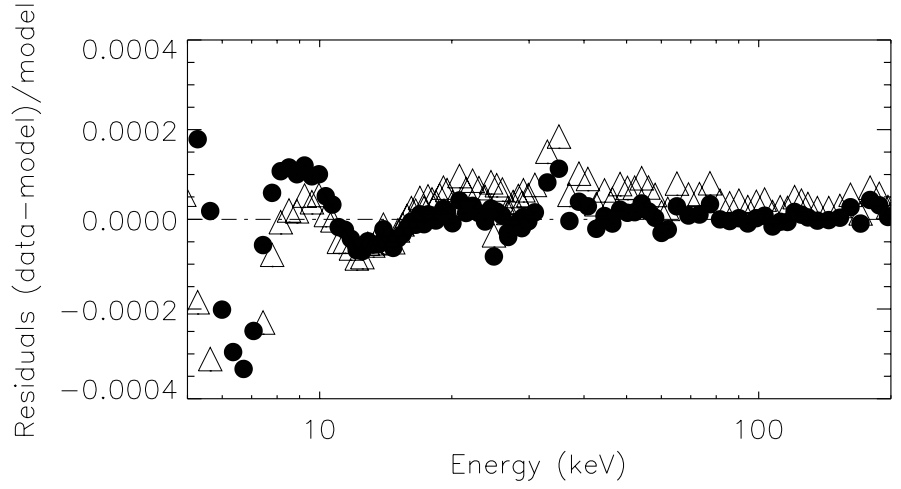

FIG. 3*b*

FIG. 3.—(*a*) Comparison between our Comptonizaton model (*solid curve*) and a simple cutoff power-law form, i.e., $\sim KE^{-\Gamma}\exp(-E/E_0)$ (*dashed curve*). Both curves resulted from fits to the overlaid data points from GX 339−4. No additional parameters (such as absorption or emission due to Fe) were included. It is evident that the Comptonization model represents the data more accurately above ~10 keV (the improvement in χ^2_ν is about 10%). As detailed in the text, we interpret the "excess" flux in that regime as being due to downscattering of hard photons in a diverging outflow. (*b*) Fit residuals (for GX 339−4) above 10 keV for the cutoff power-law model (*triangles*) and our outflow Comptonization model (*circles*). As evidenced from this figure, the downscattering effects provide a viable explanation of the 10–100 keV "excess" continuum.

residual plot. This illustrates the improvement in the fit above 10 keV. It is clear from these plots that the downscattering effects lead to an improved fit above ~10 keV. In addition, one can see the photoabsorption features below 10 keV and the higher K edge (in 7–9 keV energy band) in the residual plot (Fig. 3*a*). It is worth noting that the similar edge features along with the strong Kα lines are detected during X-ray superbursts (see Figs. 5 and 9 in Strohmayer & Brown 2002). There is a high probability that they originated in the radiation-driven outflows during burst events.

In Figure 4, we show an example of one of our model fits, in this case to GS 1353−64 (Fig. 5 is the same result, but plotted in photon space).

4. DISCUSSION

We have shown that downscattering modification of the primary photon spectrum by an outflowing plasma is a possible mechanism for producing the continuum excess in the ~10 keV spectral region. This is usually attributed to Comptonization by a static reflector, such as a downward or obliquely illuminated accretion disk, although the overall continuum form differs from that of the basic Compton reflection form. Thus we suggest that in at least some cases the outflow downscattering effect rather than the standard Compton reflection mechanism is responsible for the observed "excess" hard X-ray continuum.

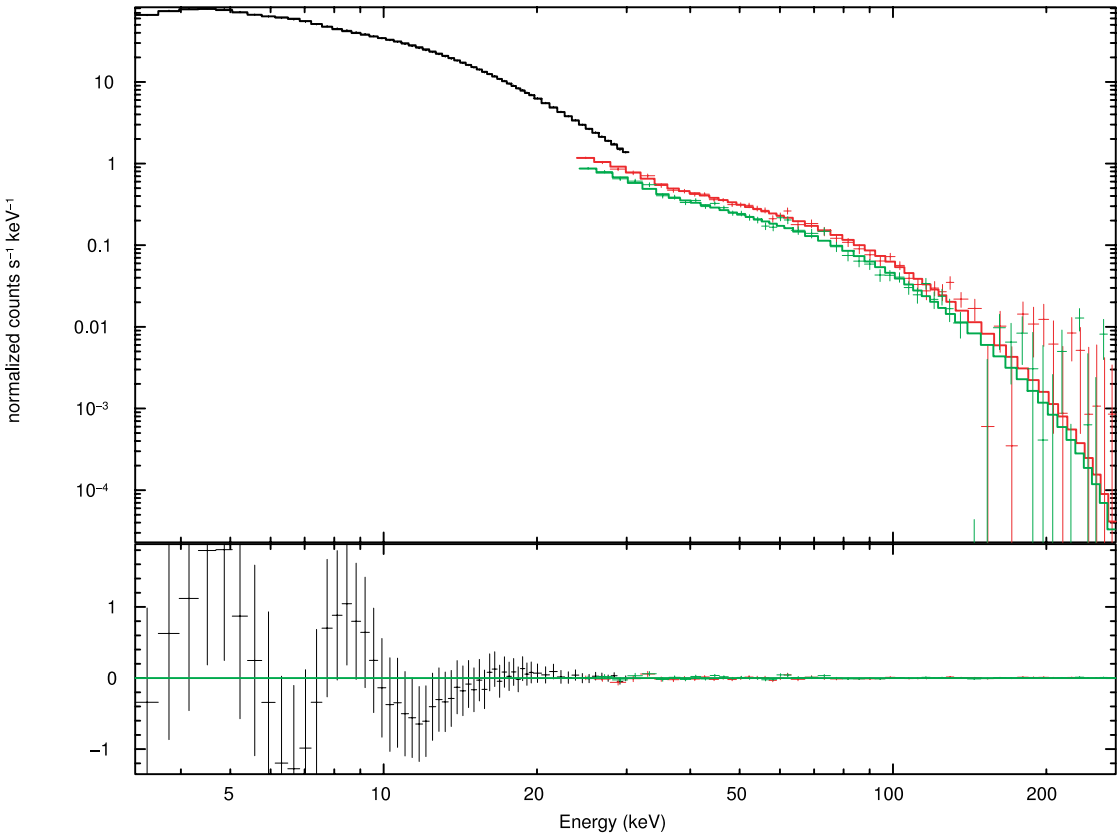

FIG. 4.—Example of the application of our model to observational data. In this case, flaring state *RXTE* data for GS 1351−64 are shown. This source has been noted by others as a strong "Compton reflection" source among the Galactic X-ray binaries. The count rate data, the folded model, and the residual are plotted. In this case, the χ^2 per degree of freedom was $\chi^2_\nu = 1.02$.

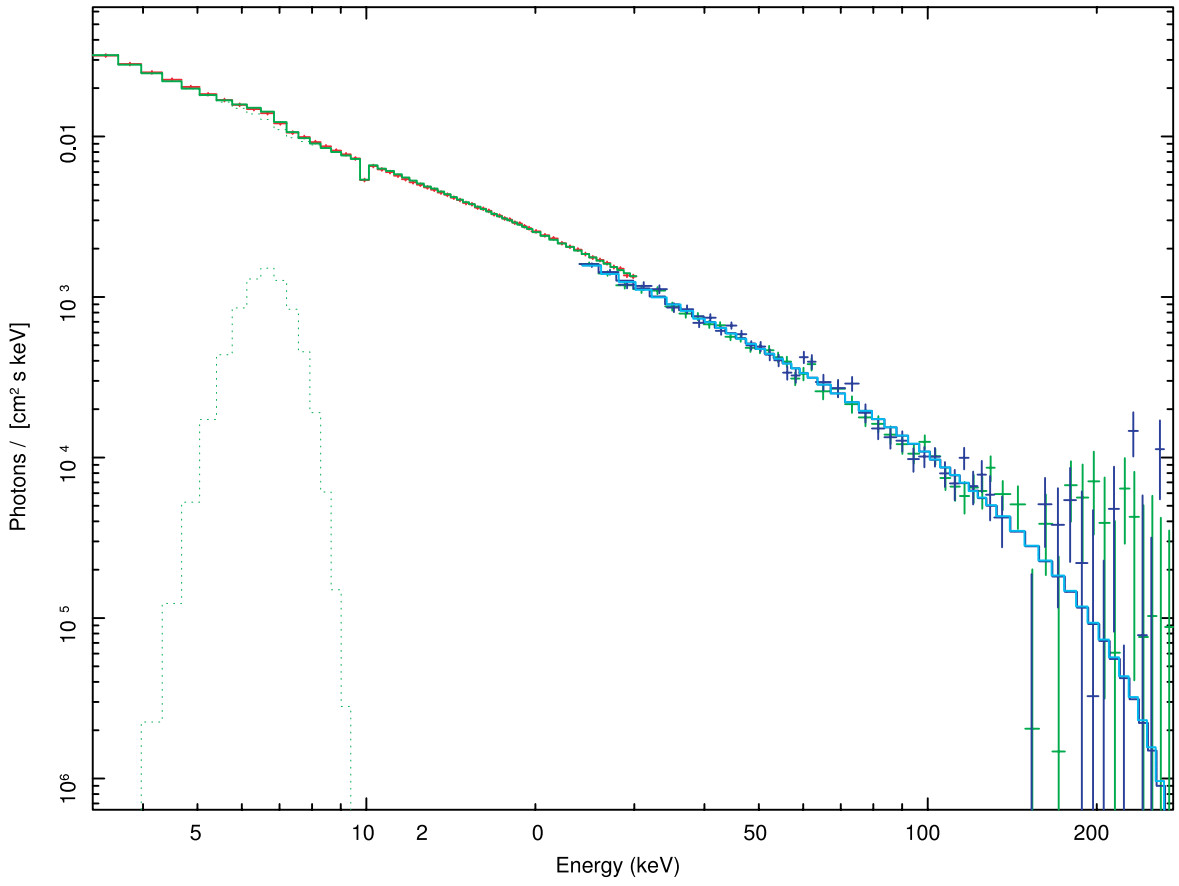

FIG. 5.—Similar to Fig. 4, but the data and model fit are plotted in photon space.

It is reasonable to expect that outflowing plasma, in the form of stellar or putative disk winds, will affect the emergent spectra of compact binaries. Collimated outflows are well known in certain objects, the so-called Galactic microquasars, and there is strong uncollimated or weakly collimated outflow in additional objects: as noted, Cyg X-3, where in fact spatially extended emission has been resolved (Heindl et al. 2003), and of course the stellar winds in Cyg X-1 have been extensively studied. Disk winds may have been observed directly in Cir X-1 (e.g., Brandt & Schulz 2000). Recently, evidence for disk winds in AGNs has emerged (e.g., Elvis 2004; Arav 2004). Further observational confirmation is needed, but if present, these winds could produce the downscattering effects we propose.

In addition to providing evidence for outflows, recent observations suggest that the putative reflector is, in at least certain objects, necessarily much larger than any reasonable disk size (e.g., Mattson & Weaver 2004; Markowitz et al. 2003). These arguments are based on temporal signatures, specifically the lack of a prompt response of the "reflected" emission to the continuum assuming light-travel times within reasonable accretion disk spatial scales. While an accretion disk torus has been suggested as an alternative, i.e., more remote, reflector, the same temporal signatures could be reproduced within the context of a central source and an ambient outflow.

We note the concerns of some authors, e.g., Miller et al. (2004), that the hot disk inner disk component and high-frequency quasi-periodic oscillations (QPOs; a few times 100 Hz) seen in accreting black holes (BHs) at the highest inferred accretion rates would not be visible through an "optically thick" outflow. Those authors thus rule out any possibility of ambient spectral reprocessing and distortion of the iron line feature, such as broadening and red-wing enhancement, by the outflow. On the other hand, LT04 infer the outflow Thomson optical depth τ_0 of the outflowing medium from parameter fitting using *XMM-Newton* and *ASCA* measurements of broad, redshifted iron lines. They find that τ_0 never exceeds 2–3 in any of the cases analyzed. Presumably, the observer sees the radiation of the BH central source through the "haze" of the moderate optical depth. Furthermore, Titarchuk et al. (2002, hereafter TCW02) give a precise model for the loss of the modulation due to photon scattering. It follows from TCW02 that the outflow optical depth $\tau_{T,0}$ would need to be around 16 or higher in order to suppress QPO amplitude of frequency 100 Hz (see formula [5] in TCW02). We have shown that this very optically thick outflow is ruled out by observations. Our results confirm the LT04 results in the sense that all effects of reprocessing and line distortion can plausibly occur in outflows characterized by moderate optical depth.

Furthermore, Laming & Titarchuk (2004) recently formulated a generic problem of the outflow illumination by the hard radiation of the central object, and they calculated the outflow temperature and ionization balance as a function of the ionization parameter. Natural assumptions regarding the X-ray spectral distribution of the central source radiation (Comptonization-like spectra) and velocity distribution in the outflow (constant velocity wind) were applied. They find that iron Kα photons are generated by the absorption of X-ray photons at energies higher than the K edge (i.e., >7 keV; see these K-edge features in Fig. 3). Electron scattering of the Kα photons within the highly ionized expanding flow leads to a decrease of their energy (redshift) that is of first order in v/c (this is clearly illustrated in Fig. 1). This photon redshift is an intrinsic property of any outflow for which the divergence is positive. Laming & Titarchuk (2004) find that the range of the parameter "inner radius/L_{40}" (which is proportional to the inverse of the so-called "ionization parameter" used in the literature) is about 10^{13} cm and the range of the wind temperature is about 10^6 K when the observed Kα lines are produced in the wind (where L_{40} is the source luminosity in 10^{40} ergs s^{-1}). They also find that the equivalent widths of red-skewed Fe Kα lines originating in the wind are on the order of 1 keV.

5. CONCLUSIONS

We have developed an analytic formulation for the emergent spectrum resulting from photon diffusion in a spherically expanding Comptonizing medium, characterized by two model parameters: an average number of scatterings in the medium $N_{\rm av}$ and the efficiency of the energy loss in the divergent flow ε. Application of the model to high-energy spectra of several compact binaries, which have been previously modeled within the Compton reflection scenarios, seems to lead to a satisfactory representation of the data. We suggest that in some instances the apparent $\sim$10 keV continuum enhancement seen in Galactic and extra galactic sources is due to downscattering effects associated with an outflow rather than to reflection by a disk.

We may also conclude that scattering and absorption of the primary line photons in the relatively "cold" outflow (in which the temperature is a few times 10^6 K) lead to the downscattering modification of the continuum and to the formation of red-skewed lines (which is a more natural and probable mechanism than the general relativistic effects in the innermost part of the accretion flow).

In future work, we will employ detailed Monte Carlo calculations to further explore the range of validity. In addition to Galactic binaries, extragalactic sources may be characterized by outflowing plasma. With the expanding database of *INTEGRAL* observations, which will hopefully lead to an increasingly accurate characterization of the high-energy continua, it may be possible to explore this idea. In addition to the continuum, we will explore the possibility of the line feature formation in the wind.

L. T. appreciates productive discussions with Philippe Laurent. L. T. also acknowledges the support of this work by the Faculty Fellowship Program in the NASA Goddard Space Flight Center. This work made use of the NASA High-Energy Astrophysics Research Archive Center (HEASARC) and the NASA *INTEGRAL* Guest Observer Facility. We also acknowledge the thorough analysis of this paper by the referee and his/her constructive and interesting suggestions.

REFERENCES

Arav, N. 2004, in ASP Conf. Ser. 311, AGN Physics with the Sloan Digital Sky Survey, ed. G. T. Richards & P. B. Hall (San Francisco: ASP), 213
Attié, D., et al. 2003, A&A, 411, L71
Basko, M. M., Sunyaev, R. A., & Titarchuk, L. G. 1974, A&A, 31, 249
Blandford, R. D., & Payne, D. G. 1981, MNRAS, 194, 1033
Brandt, W. N., & Schulz, N. S. 2000, ApJ, 544, L123
Elvis, M. 2004, in ASP Conf. Ser. 311, AGN Physics with the Sloan Digital Sky Survey, ed. G. T. Richards & P. B. Hall (San Francisco: ASP), 109
Gilfanov, M., Churazov, E., & Revnivtsev, M. 2004, in AIP Conf. Proc. 714, X-Ray Timing 2003: *Rossi* and Beyond, ed. P. Kaaret, F. K. Lamb, & J. H. Swank (New York: AIP), 97
Gilfanov, M., et al. 1999, A&A, 352, 182

Heindl, W. A., et al. 2003, ApJ, 588, L97
Laming, L. M., & Titarchuk, L. 2004, ApJ, 615, L121
Laurent, P., & Titarchuk, L. 1999, ApJ, 511, 289
———. 2001, ApJ, 562, L67
———. 2004, ApJ, submitted (LT04)
Magdziarz, P., & Zdziarski, A. 1995, MNRAS, 273, 837
Markowitz, A., Edelson, R., & Vaughan, S. 2003, ApJ, 598, 935
Mattson, B. J., & Weaver, K. A. 2004, ApJ, 601, 771
Miller, J., et al. 2004, ApJ, 601, 450
Nobili, L., Turolla, R., & Zampieri, L. 1993, ApJ, 404, 686
Nowak, M. A., Wilms, J., & Dove, J. B. 2002, MNRAS, 332, 856
Paizis, A., et al. 2003, A&A, 411, L363
Payne, D. G., & Blandford, R. D. 1981, MNRAS, 196, 781
Pottschmidt, K., et al. 2003, A&A, 411, L383
Proga, D., & Kallman, T. R. 2002, ApJ, 565, 455
Sheffer, E. K., et al. 1992, AZh, 69, 82
Still, M., et al. 2001, ApJ, 554, 352
Strohmayer, T. E., & Brown, E. F. 2002, ApJ, 566, 1045
Sturner, S., et al. 2003, A&A, 411, L81
Sunyaev, R. A., & Titarchuk, L. G. 1980, A&A, 86, 121 (ST80)
———. 1985, A&A, 143, 374 (ST85)
Titarchuk, L. 1994, ApJ, 434, 570 (T94)
Titarchuk, L., Cui, W., & Wood, P. A. 2002, ApJ, 576, L49 (TCW02)
Titarchuk, L., Kazanas, D., & Becker, P. A. 2003, ApJ, 598, 411 (TKB03)
Titarchuk, L., Mastichiadis, A., & Kylafis, N. D. 1997, ApJ, 487, 834
Vilhu, O., et al. 2003, A&A, 411, L405